Velocity-dependent screening in metals

A. F. Lifschitz and N. R. Arista
División Colisiones Atómicas, Centro Atómico Bariloche and Instituto Balseiro, Comisión Nacional de Energía Atómica, 8400 Bariloche, Argentina
(Received 21 May 1997)

We propose a model to calculate in a quantum-mechanical way the screening and energy loss of swift ions in metals. The model is based on an extension of the Friedel sum rule to finite velocities, which allows us to describe the scattering and nonlinear screening of electrons in the field of the moving ion. The scattering process is formulated according to the partial-wave expansion, assuming an effective scattering potential that is adjusted in a self-consistent way using the phase-shift sum rule. We consider in particular the limits of low and high velocities, where the results of this model agree with those obtained using the density-functional and perturbation theories. We apply the method to the calculation of the mean energy loss (stopping power) on the whole range of velocities. [S1050-2947(97)04812-9]

PACS number(s): 34.50.Bw, 34.50.Fa, 79.20.Rf

I. INTRODUCTION

The screening of ions in solids is one of the central problems in the study of ion-solid interactions. The problem is of interest to understand both the behavior of static impurities in metals, such as the resistivity of impurities and metallic solutions [1], or the energy loss and ranges of swift ions in solids [2].

Various perturbative models have been used to describe the basic interaction process. In particular, the dielectric formalism, based on linear-response theory [3–5], provides a unified description of dynamical screening, plasmon excitation, and electron-hole pairs. It shows also the main features of the velocity dependence of the stopping power of metals: a proportionality with velocity in the adiabatic low-velocity range, a threshold for plasmon excitation and maximum stopping power at intermediate velocities, and a decreasing behavior at high energies, in agreement with the Bethe theory [2]. The main weakness of this model is observed in the low-velocity range because the interaction effects become too strong to be described well by linear or perturbative approximations [6].

Models based on kinetic theory [7,8] provide also a good description of the velocity-dependent stopping power, but require a knowledge of the transport cross sections for dynamically screened interactions including quantum effects on the whole range of velocities. On the other hand, quantum-mechanical models have been proposed for the particular case of slow ions [9–16]. Briggs and Pathak [9] introduced a transport–cross-section approach based on the partial-wave method to calculate the friction coefficient for slow ions in channeling conditions. The model qualitatively explained the oscillatory dependence observed as a function of the ion atomic number Z_1. A more accurate many-body representation of the nonlinear screening and stopping process was given by Echenique *et al.* [11,12], who introduced the density-functional theory (DFT) to calculate the friction coefficient for slow ions embedded in a uniform electron gas. The model explained in a more definitive way the oscillatory Z_1 dependence for the case of channeled ions.

In order to improve the description of similar features in the case of random incidence, a simplified model to integrate the stopping power for nonhomogeneous electron distributions in solids was developed [16]. The model is strongly based on the Friedel sum rule for the phase shifts in the case of slow ions and uses this rule to adjust, in a self-consistent way, the scattering potential. The approach has been used earlier by various authors [13–15] in homogeneous systems, with very good results. The model provides a good description of both the Z_1 and the Z_2 dependences of the low-velocity friction coefficients for ions in various solid targets [16]. In addition, with a more elaborate treatment of the electronic density sampled in channeling conditions, the model was used to produce a complete simulation of the slowing down of protons channeled in Au crystals [17].

The problem of extending the quantum models to finite velocities has been considered recently either in the context of the DFT [18] or using model potentials and the Born approximation [19]. In particular, an extension of the Friedel sum rule to finite velocities is contained in the formulation given in Ref. [19]. In both cases the dynamical potential is replaced by a spherical average in order to proceed with the calculations. The model presented here also makes use of this assumption.

The purpose of this work is to extend previous models for slow ions [13–17] to the case of ions moving with arbitrary (nonrelativistic) velocities. To carry out this idea we first perform an extension of the Friedel sum rule to the case of moving ions. This extension allows us to incorporate in a self-consistent way the dynamical effects that give rise to the velocity dependence of the relevant quantities, including the behavior of the scattering terms and the energy loss of the particle. We will report here calculations performed with this model for the whole range of velocities.

The extension of the phase-shift sum rule is described in Sec. II and calculations for various velocity ranges are considered in Sec. III. The results are compared with previous models in the limits of small and large velocities. Some approximate results that may be obtained using perturbation theory are included in the Appendix.

II. MODEL

Extension of the Friedel sum rule for moving ions

Let us first consider the usual treatment of the Friedel sum rule (FSR) for static ions [20]. It may be shown in this case that each of the scattered electrons contributes to the accumulation of screening charge by an amount that, in a partial-wave expansion, is given by the derivative of the phase shift δ_l in the form $\Delta q_l=(1/\pi)(d\delta_l/dk)$. The FSR represents the condition of overall charge neutrality, expected for a metallic environment, as a result of the screening by all the electron states within a Fermi sphere. The rule may be expressed as

$$Z_1-N_b=\sum_{l,m_l,m_s}\int_0^{v_F}\left(\frac{1}{\pi}\right)\left(\frac{d\delta_l}{dk}\right)dk$$

$$=\frac{2}{\pi}\sum_{l=0}^{\infty}(2l+1)\int_0^{v_F}\left(\frac{d\delta_l}{dk}\right)dk, \tag{1}$$

where N_b is the number of bound electrons and Z_1 the nuclear charge of the ion (atomic units will be used in this paper). In this case (i.e., $v=0$) the integral over the electron velocities, or wave vectors k, extends over a Fermi sphere of radius v_F centered in the origin.

Let us consider now the case of a particle moving with velocity $\vec{v}$ along the $\hat{z}$ axis. As seen from the particle rest frame, the electrons occupy a displaced Fermi sphere whose center is located at the velocity $-\vec{v}$, while its radius v_F remains unchanged. The situation may be considered stationary in a frame of reference moving with the projectile. Moreover, in a metallic environment the intruder charge should be neutralized by the screening charge. Therefore, the condition of charge neutrality may be applied to this case.

In order to account for the ion velocity, the integration must now be preformed over a Fermi sphere displaced by $-v$ relative to the origin, as shown in Fig. 1. The contribution to the accumulation of screening charge from a spherical shell of radius k and thickness dk is given by $(1/\pi)(d\delta_l/dk)dk$; therefore, the k integration in Eq. (1) should now be replaced by an integral G_l over the displaced Fermi sphere (DFS) as

$$G_l(v,v_F)=\int_{\mathrm{DFS}}\left(\frac{d\delta_l}{dk}\right)\frac{k^2dkd\Omega}{4\pi k^2}=\int_{k_{\min}}^{k_{\max}}dk\left(\frac{d\delta_l}{dk}\right)g(k,v), \tag{2}$$

with $k_{\min}=\min\{0,v-v_F\}$ and $k_{\max}=v+v_F$. The sum rule now takes the form

$$Z_1-N_b=\frac{2}{\pi}\sum_{l=0}^{\infty}(2l+1)G_l(v,v_F). \tag{3}$$

The angular integration over the DFS, given by the function $g(k,v)$ in Eq. (2), may be performed in a simple way using the geometrical representation of the kinematics shown in Fig. 1 and taking into account the axial symmetry

$$g(k,v)=\int_{\mathrm{DFS}}\frac{d\Omega}{4\pi}=\frac{1}{2}(1-\cos\theta_c). \tag{4}$$

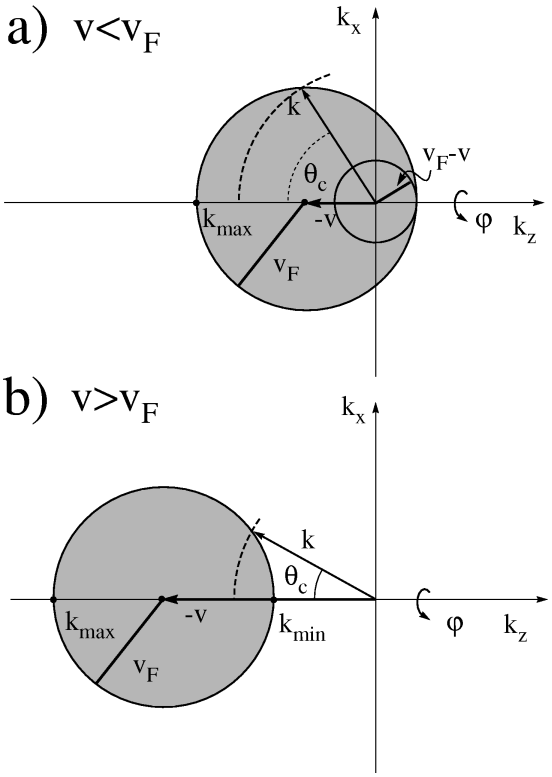

FIG. 1. Representation of the displaced Fermi sphere and integration regions for the cases (a) $v<v_F$ and (b) $v>v_F$. The maximum angle θ_c is indicated for each value of k in the Fermi sphere. For $k<v_F-v$ in case (a) the value of θ_c is π.

Here the angle θ_c corresponds to the maximum angle of the k vector for electrons in the Fermi sphere, as indicated for different cases in Fig. 1. We separate the following cases.

(a) $v<v_F$. As shown in Fig. 1(a), the integration here contains two terms, depending on the value of k: (i) $0<k<v_F-v$, in which case no restriction is applied on the angular integration and then $\theta_c=\pi$ and $g(k,v)=1$, and (ii) $v_F-v<k<v_F+v$, where $\cos\theta_c=(k^2+v^2-v_F^2)/2kv$, according to Fig. 1(a), and

$$g(k,v)=\frac{1}{4kv}[2kv+v_F^2-k^2-v^2]. \tag{5}$$

(b) $v>v_F$. This is the case shown in Fig. 1(b); we also get $\cos\theta_c=(k^2+v^2-v_F^2)/2kv$ (with $v-v_F<k<v+v_F$) and $g(k,v)$ is given again by Eq. (5).

Therefore, the extended sum rule for any velocity v becomes

$$Z_1=\frac{2}{\pi}\sum_{l=0}^{\infty}(2l+1)G_l(v,v_F)+N_b, \tag{6}$$

where

$$G_l(v,v_F)=\begin{cases}G_l^{(1)}(v,v_F)+G_l^{(2)}(v,v_F), & v<v_F\\ G_l^{(2)}(v,v_F), & v>v_F,\end{cases} \tag{7}$$

with

$$G_l^{(1)}(v,v_F)=\int_0^{v_F-v} dk\left(\frac{d\delta_l}{dk}\right)=\delta_l(v_F-v)-\delta_l(0) \quad (8)$$

and

$$G_l^{(2)}(v,v_F)=\int_{|v-v_F|}^{v+v_F} dk\left(\frac{d\delta_l}{dk}\right)g(k,v). \quad (9)$$

An alternative expression for $G_l^{(2)}$ may be obtained by partial integration

$$G_l^{(2)}(v,v_F)=\int_{|v-v_F|}^{v+v_F} dk\left[\frac{k^2+v_F^2-v^2}{4k^2v}\right]\delta_l(k), \\ -\Theta(v_F-v)\,\delta_l(v_F-v), \quad (10)$$

where $\Theta(v_F-v)$ denotes the Heaviside function. In particular, for $v=0$, $G_l^{(2)}(v,v_F)\to 0$ and the sum rule takes the simple form

$$Z_1=\frac{2}{\pi}\sum_l (2l+1)[\delta_l(v_F)-\delta_l(0)]+N_b. \quad (11)$$

Furthermore, if we use Levinson's theorem $(2/\pi)\Sigma_l(2l+1)\delta_l(0)=N_b$, the last two terms in Eq. (11) cancel out and we retrieve the Friedel sum rule in the usual form

$$Z_1=\frac{2}{\pi}\sum_l (2l+1)\,\delta_l(v_F). \quad (12)$$

In the opposite limit of $v\gg v_F$, we calculate the value of $G_l^{(2)}(v,v_F)$ using Eq. (5) in Eq. (9) and we expand the terms in powers of (v_F/v). Thus we get the result

$$Z_1\cong\left(\frac{v_F^3}{3v^2}\right)\frac{2}{\pi}\sum_l (2l+1)\left[\frac{d\delta_l}{dk}\right]_{k=v}+N_b. \quad (13)$$

III. MODEL CALCULATIONS

In order to consider the application of the extended sum rule, we study the velocity dependence of the stopping force on a moving particle. We performed calculations using two models for the interaction potential: a hydrogenic potential $V_H(r)$ and the Yukawa potential $V_Y(r)$, given respectively by

$$V_H(r)=-Z_1\left(\frac{1}{r}+\frac{\alpha}{2}\right)\exp(-\alpha r), \quad (14)$$

$$V_Y(r)=-\frac{Z_1}{r}\exp(-\alpha r). \quad (15)$$

Here α is a velocity-dependent parameter whose value was adjusted in a self-consistent way using the requirement that the calculated phase shifts δ_l should satisfy the velocity dependent sum rule of Eq. (6). The phase shifts were numerically determined by integration of the radial Schrödinger equation for each value of α and adjusting this value until the sum rule was satisfied.

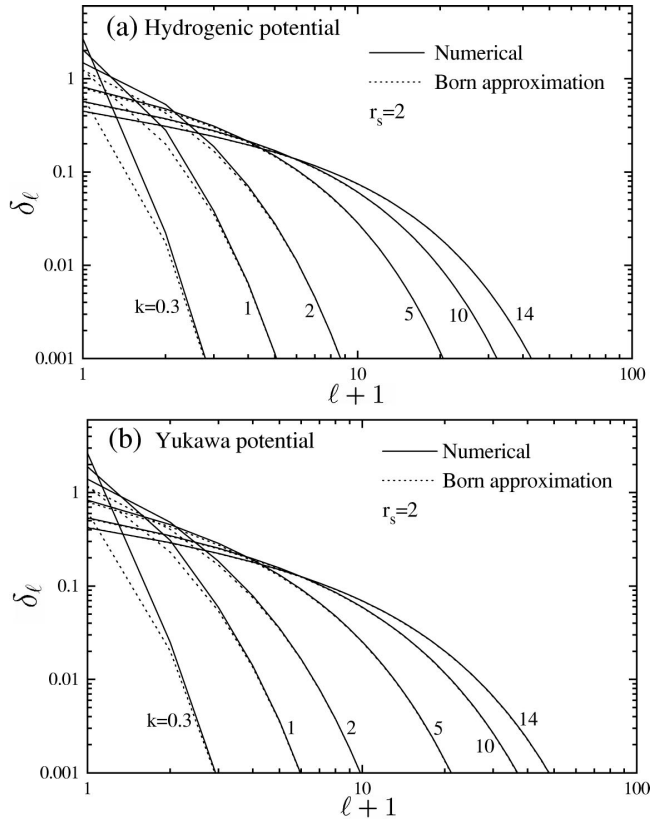

FIG. 2. Calculated values of phase shifts for (a) hydrogenic and (b) Yukawa potentials for the case $r_s=2$ (with the value of α adjusted using the FSR). Calculations for various electron velocities k as a function of $l+1$. The dotted lines show the values calculated using the Born approximation.

The main assumption on the scattering potential is that of spherical symmetry, which allows us to apply the usual phase-shift analysis. We expect that the use of the sum rule to adjust the parameter α will give us a good spherical-average representation of the real (anisotropic) potential. The goodness of this assumption will be tested later in the more unfavorable case of high velocities.

Calculations were performed for static and moving ions with nuclear charge $Z_1=2$. We will discuss first the better-known case of zero velocity and then analyze the whole velocity dependence.

A. Calculations of δ_l values for $v=0$

As a first step we have calculated the values of the phase shifts $\delta_l(k)$ for the cases of hydrogenic and Yukawa potentials; these calculations were performed by numerically solving the radial Schrödinger equation using standard methods [21,22]. We show some of the results in Figs. 2(a) and 2(b), where the δ_l values are plotted as a function of $l+1$. In both cases we have fixed the r_s parameter (related to the Fermi velocity by $v_F=1.919/r_s$) at the value $r_s=2$ (in the range of interest for several metals), while the corresponding values of α for each potential were determined by the Friedel sum-rule method, Eq. (11), using the δ_l values calculated at the Fermi surface $k=v_F$. The N_b value in this case, as determined by the Levinson sum, is $N_b=2$. As may be observed, for small values of k only a few phase shifts are needed to calculate

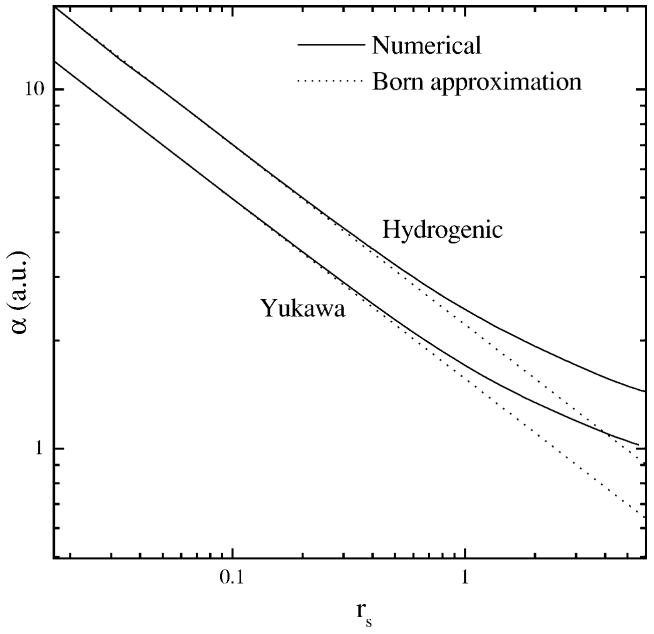

FIG. 3. Values of α obtained from the FSR (in the static case) for the hydrogenic and Yukawa potentials as a function of the electron-gas parameter r_s.

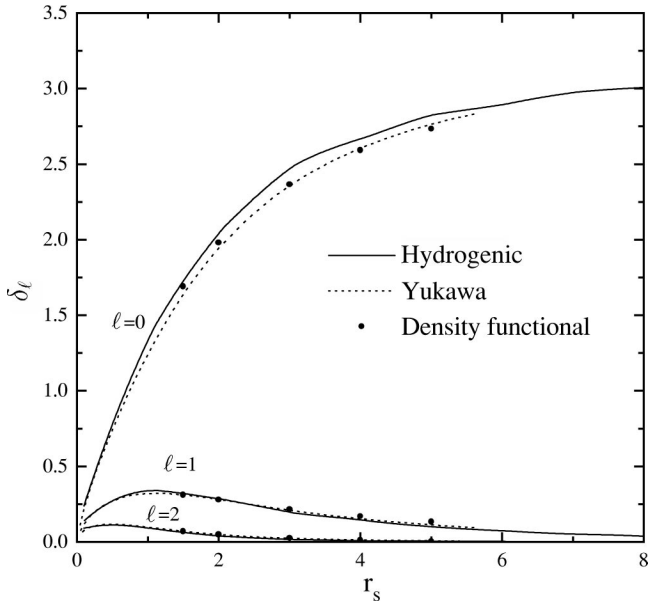

FIG. 4. Comparison of the phase shifts calculated by the present method with the values obtained from density-functional calculations (from Ref. [23]).

the cross section, but with increasing k the δ_l curves flatten and the number of phase shifts required increases accordingly. We also show in these figures the phase shift values calculated from the Born approximation (see the Appendix). We find that the Born results give a very good approximation for electron velocities larger than about 2 and for l values also larger than ~ 2.

In Fig. 3 we show the values of α for the case of fixed ions ($v=0$), obtained by adjusting the Friedel sum rule (12) for both potentials. The dotted lines show the values expected by using the Born approximation (Appendix); these values approach the exact results in the limit of small r_s (i.e., large v_F), similarly to the behavior observed at high electron velocities in Fig. 2. The perturbative approximations apply well both in the high-velocity and in the high-density [the so-called random-phase approximation (RPA)] limits.

Finally, in Fig. 4 we compare the values calculated here with those obtained using the density-functional method [23]. We find good agreement with these values for the hydrogenic potential and very good agreement for the Yukawa potential.

B. Velocity dependence

We now turn to the ion-velocity dependence of the model presented here. As already indicated, we use a self-consistent method where the screening effects are represented in a simple form using a model potential with a single parameter α, which now becomes a function of the ion velocity and whose value is determined by the application of the velocity-dependent sum rule. For the present calculations we assume a bare ion, with $Z_1=2$ and $N_b=0$.

The calculations were performed using Eqs. (6)–(10), starting at very low velocities with the α values determined for static ions (with $Z_1=2$, $N_b=0$) and searching for the new values of α by an iteration procedure. As the velocity increases, more phase shifts δ_l must be incorporated into the sum rule. At the largest velocities considered here (~ 10) up to 600 values of l were included. However, for $l \gg 1$, we have used the analytical results provided by the Born approximation to speed up the iteration process.

The values of α obtained in this way are shown in Fig. 5 for each of the potentials. The dotted lines show the asymptotic α values (α_B) derived by using only the Born approximation in the high-velocity form of the sum rule (13). These limiting values can be calculated analytically using the

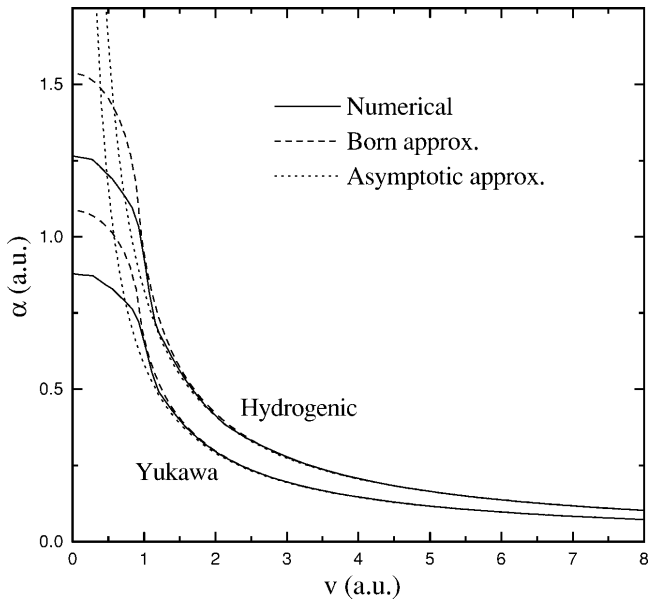

FIG. 5. Velocity dependence of the screening parameter α for $r_s=2$. Solid lines, numerical values obtained from the extended sum rule (6) for both the hydrogenic and Yukawa potentials; dotted lines, high-velocity approximation ($v \gg v_F$) from Eq. (18); dashed lines, velocity-dependent α values in the linear approximation of Eq. (19).

fact that in the Born approximation the δ_l^B values satisfy the linearized sum rule (see the Appendix)

$$\frac{2}{\pi}\sum_l (2l+1)\,\delta_l^B(k)=\frac{4k}{\pi}\,\frac{\gamma Z_1}{\alpha_B^2}, \tag{16}$$

with $\gamma=1$ for the Yukawa potential and $\gamma=2$ for the hydrogenic potential.

Using these values in Eq. (13) (with $N_b=0$) we get, in the high-velocity limit,

$$Z_1=\left(\frac{v_F^3}{3v^2}\right)\left[\frac{d}{dk}\left(\frac{4k}{\pi}\,\frac{\gamma Z_1}{\alpha_B^2}\right)\right]_{k=v}=\left(\frac{4v_F^3}{3\pi v^2}\right)\frac{\gamma Z_1}{\alpha_B^2} \tag{17}$$

and therefore

$$\alpha_B\cong\gamma^{1/2}\frac{\omega_P}{v}, \tag{18}$$

with the values of γ indicated before for each case. We have used here the relation $v_F^3=(3\pi/4)\omega_P^2$ between v_F and the plasma frequency ω_P.

On the other hand, one can obtain an extended analytical expression for α by using the limiting condition of Eq. (16) in the exact expressions of Eqs. (6) and (10) [i.e., by inserting the sum over l values in Eq. (6) within the integral of Eq. (10) and making use of Eq. (16)]. In this case the integral may be handled analytically and one obtains an approximation for α that has a more appropriate velocity dependence, viz.,

$$\alpha_B^2(v)=\gamma\frac{2v_F}{\pi}\left[1+\frac{v_F^2-v^2}{2v_Fv}\ln\left|\frac{v+v_F}{v-v_F}\right|\right]. \tag{19}$$

This expression applies to any screened potential of the form $V(r)=-(Z_1/r)\Phi(\alpha r)$, with the value of γ given by Eq. (A11) in the Appendix. In particular, for the case of a Yukawa potential Eq. (19) coincides with the one derived by Nagy and Bergara [19] also in the linear approximation. The velocity dependence of the α values obtained from this expression are shown with dashed lines in Fig. 5; these values are in better agreement with the numerical results (solid lines) for intermediate and large velocities, but they deviate from the exact values in the low-velocity regime, where nonlinear effects become important.

We parenthetically note that the α values for $v=0$ shown in Fig. 5 differ from those of Fig. 3 for the case $r_s=2$. This is due to the assumption of different N_b values in both cases. The calculations for static ions in Fig. 3 are consistent with the value $N_b=2$ resulting from Levinson's theorem for this case, whereas those in Fig. 5 were made under the assumption of $N_b=0$, i.e., the expected value for fast ions. A realistic simulation of helium ions in matter would involve a combination of the different charge states ($N_b=0$, 1, and 2) with the statistical weights determined by dynamical effects and capture and loss processes [24].

As a final remark, the dependence on ω_P/v in Eq. (18) is the typical one for the high-velocity limit (dynamical-screening distance $\sim v/\omega_P$) when the collective behavior of a free-electron gas is considered. One should note, however, that collective effects have not been explicitly included in this description; they arise in our case as a result of the self-consistency imposed by the model (through the sum-rule requirement). A similar appearance of collective behavior in a velocity-dependent density-functional description has been discussed by previous authors [18].

C. Velocity-dependent stopping power

As an application of the method we consider the calculation of the stopping force $S(v)\equiv -dE/dx$ for ions moving in a metal. A simple and yet nontrivial question here is whether the present description of nonlinear screening describes the well-known existence of a maximum in the energy loss for ion velocities close to the electron Fermi velocity as well as the high-velocity behavior.

To integrate the average energy loss we use a previously derived expression, based on a transport–cross-section description of the process [8], which gives the stopping power as an integral of $\sigma_{\rm tr}$ in the form

$$S(v)=\frac{1}{4\pi v^2}\int_0^{v_F}u\,du\int_{|v-u|}^{|v+u|}dk\;k^4\sigma_{\rm tr}(k,v)\left[1+\frac{v^2-u^2}{k^2}\right]. \tag{20}$$

This expression takes into account the statistical average of the momentum transfers due to collisions with relative velocities $v_r\equiv k$ (in the range $|v-u|<k<|v+u|$), between the moving ion (with velocity v), and a distribution of electrons incident from all angles and with all possible velocities u inside the Fermi sphere ($0<u<v_F$), as shown in Fig. 1.

The transport cross section $\sigma_{\rm tr}(k,v)$ is calculated according to the usual expression (for a relative electron-ion velocity $v_r=k$)

$$\sigma_{\rm tr}(k,v)=\frac{4\pi}{k^2}\sum_{l=1}^{\infty}(l+1)\sin^2[\,\delta_l(k)-\delta_{l+1}(k)]. \tag{21}$$

The dependence on ion velocity v is implicitly considered through the phase shifts $\delta_l(k)$, whose values depend parametrically on the ion velocity v because of the requirement imposed by the velocity-dependent sum rule used to adjust the potential $V(r)$ [with $\alpha=\alpha(v)$] as described before.

The stopping power values obtained in this way are shown in Fig. 6 together with the expected limits from the low- and high-velocity regimes. The former is given by the low-velocity stopping coefficient [10]

$$S_{\rm low}(v)=nvv_F\sigma_{\rm tr}(v_F), \tag{22}$$

while the latter is given by a Bethe-like formula [2], as shown in the Appendix,

$$S_{\rm high}(v)\cong\frac{Z_1^2\omega_P^2}{v^2}\ln\left(\frac{2mv}{\hbar\alpha}\right)\cong\frac{Z_1^2\omega_P^2}{v^2}\ln\left(\frac{2mv^2}{\hbar\omega_P}\right). \tag{23}$$

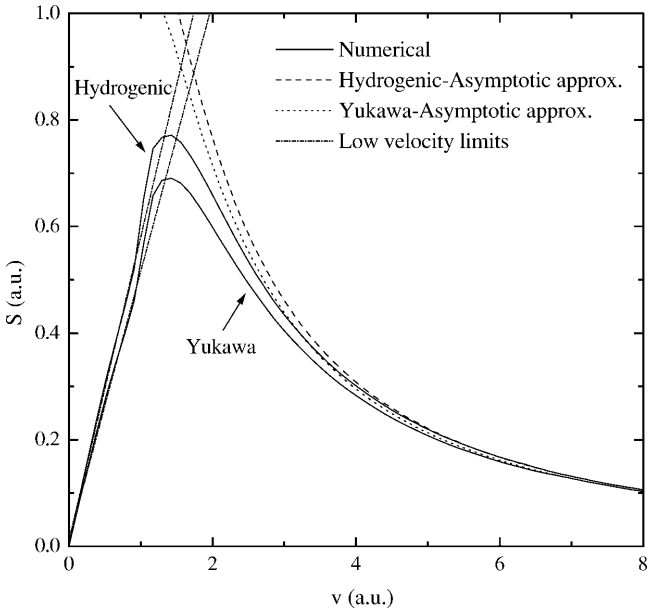

FIG. 6. Velocity dependence of the energy loss (stopping power) for α particles in a free electron gas (with $r_s=2$). The dotted lines show the low- and high-velocity limits described in the text.

Here we have used the high-velocity (perturbation) limit of the α values ($\alpha \sim \omega_P/v$) arising from the sum-rule method, which in this limit correspond to dynamical-screening effects typically found in the range of plasmon behavior (the standard approach to obtain the high-velocity result includes the contribution of single-particle and plasmon excitations [2]).

As may be observed, the present model joins in a smooth way the limiting cases and produces the maximum in the stopping power. The largest difference between the results for the hydrogenic and Yukawa potentials is about 10% for intermediate velocities.

IV. CONCLUSIONS

We have proposed a model to describe the velocity-dependent screening in metals based on the extension of the Friedel sum rule to finite velocities and on the use of this rule to adjust in a self-consistent way the parameters of simple analytical potentials. The model provides a simple way to incorporate dynamical effects in the quantum formulation of screening and scattering processes, which is considered an appropriate framework to analyze nonlinear screening and stopping powers of ions in metals.

In the low-velocity limit the present model coincides with the previous adiabatic picture of a friction force produced by the scattering of electrons in the field of a nearly static ion. In this range, the results are in good agreement with those obtained from the density-functional formulation. In the high-velocity limit our results agree with perturbative expansions leading to the well-known Bethe formula.

The special interest of this model is that it may be applied in the more complicated range of intermediate velocities, bridging the existing gap between previous linear and nonlinear models. In this intermediate range the results reproduce the maximum in the stopping power. This velocity dependence arises in a natural way (i.e., not by any external imposition) as a result of the self-consistent mechanism used to adjust the screening potential by the velocity-dependent sum rule.

The accuracy of the model is limited to some extent by the restriction in the potential function, which is assumed to maintain the spherical symmetry for finite velocities. However, the self-consistent optimization applied to this potential makes this assumption become less critical, as may be checked by considering the behavior of the results in the more unfavorable case of high velocities.

The model provides also the possibility to calculate the stopping powers for the different charge states (using the N_b number) in the case of moving ions. This will be used to represent the average energy loss for a beam of ions with equilibrium or nonequilibrium charge states.

ACKNOWLEDGMENT

This work was partially supported by Consejo Nacional de Investigaciones Científicas y Técnicas (Argentina).

APPENDIX

We consider here the calculation of phase shifts and transport cross sections using perturbation theory and derive related approximations to the sum rule in the high-velocity limit. Following the usual first-order Born approximation [25], the phase shifts are given by

$$\delta_l^B(k) = -\pi \int_0^\infty dr\ r\ V(r)[J_{l+1/2}(kr)]^2. \tag{A1}$$

Thus we obtain for the Yukawa potential

$$\delta_l^{BY} = \pi Z_1 \int_0^\infty dr\ e^{-\alpha r}[J_{l+1/2}(kr)]^2 = \frac{Z_1}{k} Q_l(x) \tag{A2}$$

and for the hydrogenic potential

$$\delta_l^{BH} = \pi Z_1 \int_0^\infty dr\ r\ e^{-\alpha r}\left(1+\frac{\alpha r}{2}\right)[J_{l+1/2}(kr)]^2 = \begin{cases} \dfrac{Z_1}{k} Q_0(x) + \dfrac{Z_1 \alpha^2}{2k^3}\left(\dfrac{1}{x^2-1}\right), & l=0 \\ \dfrac{Z_1}{k} Q_l(x) - \dfrac{Z_1 \alpha^2}{2k^3}\left(\dfrac{1}{x^2-1}\right) l[xQ_l(x) - Q_{l-1}(x)], & l>0, \end{cases} \tag{A3}$$

where the $Q_l(x)$ are the second-kind Legendre functions of lth order [26] and

$$x=1+\frac{\alpha^2}{2k^2}. \tag{A4}$$

Using these expressions we can derive the corresponding approximations to the Friedel sum rule. Let us consider first the case of low velocities.

Using the relation [26]

$$J_{l+1/2}(z)=\sqrt{\frac{2z}{\pi}}j_l(z), \tag{A5}$$

we may write Eq. (A1) in the form

$$\delta_l^B=-2k\int_0^\infty dr\ r^2V(r)j_l^2(kr) \tag{A6}$$

and the FSR (for $v=0$, $k=v_F$) may be written

$$\begin{aligned}Z_1&\cong\frac{2}{\pi}\sum_{l=0}^{\infty}(2l+1)\delta_l^B(v_F)\\&=-\frac{4v_F}{\pi}\int_0^\infty dr\ r^2V(r)\sum_{l=0}^{\infty}(2l+1)j_l^2(v_Fr).\end{aligned} \tag{A7}$$

Using here the property [26]

$$\sum_{l=0}^{\infty}(2l+1)j_l^2(kr)=1, \tag{A8}$$

we get the simple condition

$$Z_1\cong-\frac{4v_F}{\pi}\int_0^\infty dr\ r^2V(r), \tag{A9}$$

where the integral can be calculated for any screened potential of the form $V(r)=-(Z_1/r)\Phi(\alpha r)$, thus obtaining

$$\int_0^\infty dr\ r^2V(r)=-\gamma\frac{Z_1}{\alpha^2}, \tag{A10}$$

with a numerical constant

$$\gamma=\int_0^\infty dx\ x\ \Phi(x). \tag{A11}$$

In particular, one gets $\gamma=1$ for the Yukawa potential and $\gamma=2$ for the hydrogenic potential. Therefore, the FSR in the perturbation limit takes a very simple form

$$Z_1\cong\frac{2}{\pi}\sum_{l=0}^{\infty}(2l+1)\delta_l^B(v_F)=\frac{4v_F}{\pi}\frac{\gamma Z_1}{\alpha^2}. \tag{A12}$$

According to this relation, the values of α that would be consistent with both the Friedel sum rule and the Born approximations (with a strong assumption on the validity of the Born approximation in the low-velocity case), are given by

$$\alpha_H=\sqrt{\frac{8v_F}{\pi}}=\sqrt{6}\frac{\omega_P}{v_F}, \tag{A13}$$

$$\alpha_Y=\sqrt{\frac{4v_F}{\pi}}=\sqrt{3}\frac{\omega_P}{v_F} \tag{A14}$$

for the hydrogenic and Yukawa potentials, respectively.

We note that the value of α_Y coincides with the so-called Thomas-Fermi approximation (or RPA) to the screening constant for static ions in a free electron gas [5], namely, $k_{TF}=\sqrt{3}\omega_P/v_F$, whereas the value of α_H is a factor $\sqrt{2}$ larger.

In a similar way, we may consider the high-velocity limit, where $k=v$, and make a similar derivation. We start now from Eq. (13), which we write as

$$Z_1-N_b\cong\frac{v_F^3}{3v^2}\frac{d}{dk}\left[\frac{2}{\pi}\sum_l(2l+1)\delta_l^B(k)\right]\Bigg|_{k=v}. \tag{A15}$$

Using again Eqs. (A1) and (A8), we get

$$\frac{2}{\pi}\sum_l(2l+1)\delta_l^B(k)=-\frac{4k}{\pi}\int_0^\infty dr\ r^2V(r); \tag{A16}$$

from Eqs. (A10), (A15), and (A16),

$$Z_1-N_b\cong\frac{4v_F^3}{3\pi v^2}\frac{\gamma Z_1}{\alpha^2}=\frac{\omega_P^2}{v^2}\frac{\gamma Z_1}{\alpha^2}, \tag{A17}$$

with the values of γ given above. This equation determines the value of α for each potential in the high-velocity limit. In particular, for bare ions ($N_b=0$) we get the simple result

$$\alpha=\gamma^{1/2}\frac{\omega_P}{v}, \tag{A18}$$

which corresponds to the usual behavior of the dynamical screening of swift ions in an electron gas [3,4].

Let us finally derive the asymptotic behavior of the transport cross section and stopping powers in the limit of high velocities. The scattering amplitude $f(\theta)$ in the first-order Born approximation is given by

$$f^B(\theta)=\int d^3r\frac{\sin(qr)}{qr}V(r). \tag{A19}$$

For the hydrogenic (H) and Yukawa (Y) potentials indicated above, we obtain

$$\begin{aligned}f^{BH}(\theta)&=4\pi Z_1\frac{q^2+2\alpha^2}{(q^2+\alpha^2)^2},\\f^{BY}(\theta)&=\frac{4\pi Z_1}{q^2+\alpha^2},\end{aligned} \tag{A20}$$

where $q=2k\sin(\theta/2)$. Then we calculate the transport cross section, given by

$$\sigma_{\rm tr}=\int d\Omega|f(\theta)|^2(1-\cos\theta), \tag{A21}$$

and we get for each case

$$\sigma_{\rm tr}^{BH}(k)=2\pi\frac{Z_1^2}{k^4}\left\{\ln(q^2+\alpha^2)-\frac{q^2\alpha^2}{(q^2+\alpha^2)^2}-\frac{\alpha^4}{6}\left[\frac{1}{(q^2+\alpha^2)^2}+\frac{2q^2}{(q^2+\alpha^2)^3}\right]\right\}\Bigg|_{q_{\rm min}}^{q_{\rm max}}, \tag{A22}$$

$$\sigma_{\rm tr}^{BY}(k)=2\pi\frac{Z_1^2}{k^4}\left[\ln(q^2+\alpha^2)+\frac{\alpha^2}{(q^2+\alpha^2)}\right]\Bigg|_{q_{\rm min}}^{q_{\rm max}}, \tag{A23}$$

where $q_{\rm min}=0$ and $q_{\rm max}=2k$. In the high-velocity limit, the stopping power $S=-dE/dx$ is directly given by $\sigma_{\rm tr}(v)$ through the relation

$$S=nv^2\sigma_{\rm tr}(v). \tag{A24}$$

Therefore, using Eqs. (A22) and (A23) and considering the limit $q_{\rm max}=2v\gg\alpha$, we finally obtain

$$S(v)\cong 4\pi n\frac{Z_1^2}{v^2}\ln\left(\frac{2v}{\alpha}\right), \tag{A25}$$

which, with the corresponding values of α given in Eq. (A18), provides the expected behavior in the $v\gg v_F$ limit.

[1] N. F. Mott and H. Jones, *The Theory of the Properties of Metals and Alloys* (Dover, New York, 1958).

[2] M. A. Kumakhov and F. F. Komarov, *Energy Loss and Ion Ranges in Solids* (Gordon and Breach, New York, 1981).

[3] J. Lindhard, K. Dan. Vidensk. Selsk. Mat. Fys. Medd. **28**, 8 (1954).

[4] D. Pines, *Elementary Excitations in Solids* (Benjamin, New York, 1963).

[5] C. Kittel, *Quantum Theory of Solids* (Wiley, New York, 1987).

[6] P. M. Echenique and M. E. Uranga, in *Interaction of Charged Particles with Solids and Surfaces*, edited by A. Gras-Martí, H. M. Urbassek, N. R. Arista, and F. Flores (Plenum, New York, 1991).

[7] P. Sigmund, Phys. Rev. A **26**, 2497 (1982).

[8] L. De Ferrariis and N. R. Arista, Phys. Rev. A **29**, 2145 (1984).

[9] J. S. Briggs and A. P. Pathak, J. Phys. C **6**, L153 (1983); **7**, 1929 (1974).

[10] T. L. Ferrell and R. H. Ritchie, Phys. Rev. B **16**, 115 (1977).

[11] P. M. Echenique, R. M. Nieminen, and R. H. Ritchie, Solid State Commun. **37**, 779 (1981).

[12] P. M. Echenique, R. M. Nieminen, J. C. Ashley, and R. H. Ritchie, Phys. Rev. A **33**, 897 (1986).

[13] P. F. Meier, Helv. Phys. Acta **48**, 227 (1975).

[14] A. Ventura, Nuovo Cimento **10D**, 43 (1988).

[15] B. Apagyi and I. Nagy, J. Phys. C **20**, 1465 (1987).

[16] J. Calera Rubio, A. Gras-Martí, and N. R. Arista, in *Ionization of Solids by Heavy Particles*, edited by R. A. Baragiola (Plenum, New York, 1993); Nucl. Instrum. Methods Phys. Res. B **93**, 137 (1994).

[17] P. Vargas, J. E. Valdés, and N. R. Arista, Phys. Rev. A **53**, 1638 (1996).

[18] E. Zaremba, A. Arnau, and P. M. Echenique, Nucl. Instrum. Methods Phys. Res. B **96**, 619 (1995).

[19] I. Nagy and A. Bergara, Nucl. Instrum. Methods Phys. Res. B **115**, 58 (1996).

[20] J. Friedel, Philos. Mag. **43**, 153 (1952); Adv. Phys. **3**, 446 (1954).

[21] F. Calogero, *Variable Phase Approach to Potential Scattering* (Academic, New York, 1967).

[22] F. Salvat and R. Mayol, Comput. Phys. Commun. **62**, 65 (1991).

[23] M. J. Puska and R. M. Nieminen, Phys. Rev. B **27**, 6121 (1983).

[24] A. Arnau, M. Peñalba, P. M. Echenique, F. Flores, and R. H. Ritchie, Phys. Rev. Lett. **65**, 1024 (1990).

[25] L. D. Landau and E. M. Lifshitz, *Quantum Mechanics* (Pergamon, New York, 1977).

[26] *Handbook of Mathematical Functions*, edited by M. Abramowitz and I. A. Stegun (Dover, New York, 1970).